



Measurement of attack transients in a clarinet driven by a ramp-like varying pressure

Baptiste Bergeot, André Almeida, Christophe Vergez, Bruno Gazengel

► To cite this version:

Baptiste Bergeot, André Almeida, Christophe Vergez, Bruno Gazengel. Measurement of attack transients in a clarinet driven by a ramp-like varying pressure. Acoustics 2012, Apr 2012, Nantes, France. hal-00810986

HAL Id: hal-00810986

<https://hal.science/hal-00810986>

Submitted on 23 Apr 2012

HAL is a multi-disciplinary open access archive for the deposit and dissemination of scientific research documents, whether they are published or not. The documents may come from teaching and research institutions in France or abroad, or from public or private research centers.

L'archive ouverte pluridisciplinaire **HAL**, est destinée au dépôt et à la diffusion de documents scientifiques de niveau recherche, publiés ou non, émanant des établissements d'enseignement et de recherche français ou étrangers, des laboratoires publics ou privés.



Measurement of attack transients in a clarinet driven by a ramp-like varying pressure

B. Bergeot^a, A. Almeida^a, C. Vergez^b and B. Gazengel^a

^aLaboratoire d'acoustique de l'université du Maine, Bât. IAM - UFR Sciences Avenue Olivier Messiaen 72085 Le Mans Cedex 9

^bLMA - CNRS (UPR 7051), 31 chemin Joseph-Aiguier, 13402 Marseille, Cedex 20, France
baptiste.bergeot.etu@univ-lemans.fr

We investigate the influence of a time-varying blowing pressure on the oscillation threshold and attack transient of a clarinet. In this experimental study, a clarinet-like instrument is blown through an artificial mouth, which allows the time profile of the blowing pressure to be controlled during the experiment. The chosen profile is a slowly increasing and decreasing linear ramp. Different experiments have been carried out and analyzed. Depending on the slope of the ramp, the oscillation threshold and the attack transient are determined. To find out if the fact that the blowing pressure varies in time have a similar influence on a real clarinet as on a simplified mathematical model the experimental results are compared to the conclusions presented in a companion paper where a mixed numerical/analytical approach has been developed on a simplified mathematical model of clarinet. Characteristics such as bifurcation delay and dynamic bifurcation are addressed.

1 Introduction

Clarinet-like instruments have been thoroughly studied in the literature. In particular, a simple model assuming that losses in the cylindrical pipe are frequency independent (the so-called "Raman's model"), allows to predict the mouth pressure required to create the self-sustained oscillations [1]. This particular value of the mouth pressure is called *oscillation threshold*. Comparison between theoretical oscillation threshold and its experimental value is sometimes good [2] but sometimes the difference can reach several tens of percent [3] even using more sophisticated models [4]. The inherent difficulties of the comparison between theoretical threshold and its experimental value are studied in [5].

One of the reasons which can explain this difference between the theoretical oscillation threshold and its experimental value is the intrinsic difference between the system described by the usual theory and the one used in experiments. Indeed, the oscillation threshold measurement consists in starting from 0 the mouth pressure and to increase it until oscillations start. This is a *dynamic* case because the blowing pressure increases over time. On the other hand, the theory considers the system in a *static* case: the blowing pressure is constant. This theory is called *static* bifurcation theory and the theoretical oscillation threshold is called *static* oscillation threshold.

Recent mathematical and physical works [6, 7, 8] about analytical description of dynamical nonlinear systems shows that, in dynamic cases (as in experiments), the oscillations start significantly after the *static* theoretical threshold has been reached. This phenomenon is known under the name of *bifurcation delay* or *dynamic bifurcation*. Bifurcation delay may explain why measured thresholds are often larger than their *static* theoretical value.

This paper presents a first experimental study of bifurcation delay in clarinet-like systems and the influence of the time evolution of the mouth pressure on it. The results are compared to the conclusions presented in a companion paper [9] where a mixed numerical/analytical approach has been developed on a simplified mathematical model of clarinet. Before that, Section 2 introduces the simplified mathematical model of clarinet-like instruments (Raman's model). The main theoretical results from *static* bifurcation theory are reminded to make the description of the experimental results easier.

2 Model of clarinet-like instruments

The seminal article from Mc Intyre *et al.* [10] proposed a general model for self-sustained musical instruments such as the clarinet.

This model divides the instrument into two elements: the exciter and the resonator. The exciter is modeled by a nonlinear function F , also called nonlinear characteristic of the exciter, which relates pressure P to flow U [11]. The resonator (the bore of the instrument) is described by its reflection function $r(t)$.

In the case of a clarinet the coupling between the two elements allows to compute the state of the instrument throughout all values of time t . The state of the instrument model can be fully described by two variables: the pressure $P(t)$ inside the mouthpiece and the flow $U(t)$ created by the pressure imbalance between the mouth and the bore input.

The solution $P(t)$ and $U(t)$ depends on the control parameters: P_m representing the mouth pressure and ζ which characterizes the intensity of the flow. The nonlinear characteristic is provided by the Bernoulli equation describing the flow in the reed channel [12, 13].

Mathematical analysis of this model with off from the extreme simplification of considering a straight, lossless (or "Raman's model" considering losses independent of frequency) resonator and the reed as a ideal spring [14, 11, 15, 16, 1, 17]. With these assumptions, the reflection function becomes a simple delay with sign inversion (multiplied by an attenuation coefficient λ in the case of frequency independent losses). Using the variables P^+ and P^- (outgoing and incoming waves respectively) instead of the variables P and U , the system can be simply described by the following equation :

$$P^+(t) = G_\gamma (\lambda P^-(t - \tau)), \quad (1)$$

where $\tau = 2l/c$ is the round trip time of the pressure perturbation with velocity c along the resonator of length l . The iteration function G_γ is obtained by transforming the nonlinear characteristic F . An explicit expression was determined by Taillard *et al.* [18]. The expression of the attenuation coefficient λ is:

$$\lambda = e^{-2\alpha l}, \quad (2)$$

where,

$$\alpha \approx 3 \cdot 10^{-5} \sqrt{f}/R. \quad (3)$$

R is the radius of the bore: $R = 7.5 \cdot 10^{-3}$ m in our experiment and f is the frequency in Hz.

A study of the stability of the fixed points of the function G_γ , based on the usual static bifurcation theory (i.e. assuming that the mouth pressure is constant along the time), gives an analytical expression P_{mt} of the static oscillation threshold [19]:

$$P_{mt} = \frac{1}{9} \left(\frac{\tanh(\alpha l)}{\zeta} + \sqrt{3 + \left(\frac{\tanh(\alpha l)}{\zeta} \right)^2} \right)^2 P_M, \quad (4)$$

where P_M is the static closing pressure of the reed and ζ is a nondimensional parameter ; its expression is :

$$\zeta = Z_c S \sqrt{\frac{2}{\rho P_M}}, \quad (5)$$

where S is the opening cross-section of the reed channel at rest, ρ the density of the air and Z_c is the characteristic impedance of the resonator.

To summary, we can say that the *static* bifurcation theory, is restricted to the steady state. It can predict the asymptotic (or *static*) behavior of an ideal clarinet as a function of a constant mouth pressure. In other words, the results are obtained by choosing a value of γ , letting the system relax to its final state, and repeating the procedure for each value of γ .

3 Experimental setup : the pressure controlled artificial mouth

The experimental results presented in Section 4.2 are obtained thanks to a controlled artificial mouth [20, 21]. The artificial mouth consists of a Plexiglas box. The mouthpiece and the barrel are fixed in the box. Resonators (for example, a real clarinet or a simple cylinder as in our experiment¹) can be fixed onto the other end of the barrel (see Figure. 1).

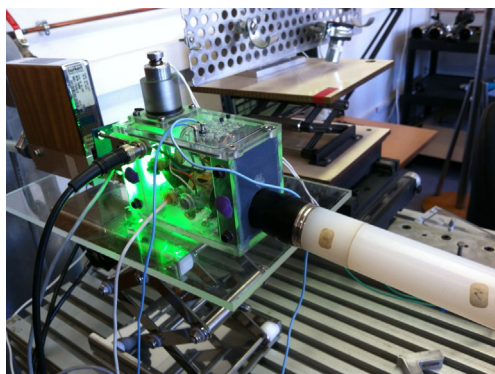


Figure 1: General view of the artificial mouth.

The machinery of the controlled artificial mouth is based on a high-precision regulation of the air pressure in the Plexiglas box. What is meant by regulation is the control of the blowing pressure around a target: a fixed value or around a value whose evolution in time is slow (like slowly varying ramps as in this present work). The experimental setup is presented in Figure 2.

A servo-valve is connected to a compressed air source through a pressure reducer. The maximum pressure available is around 6 bars, and the pressure reducer is used to adjust the pressure P_1 upstream the servo-valve. The servo-valve is connected to the entrance of the artificial mouth itself (whose 30 cm³ internal volume is the place where the air pressure P_m is to be controlled). The artificial mouth blows into the clarinet. An air tank (120L) has been added between the servo-valve and the artificial mouth (not represented in Figure 2) in order to stabilize the feedback loop during onsets.

The principle of the control is as follows: through a control algorithm implemented on a DSP card, the volume flow through the servo-valve is modified every 40 μ s in order to

¹We use a plastic cylinder, its length is $l = 0.51$ m including the barrel.

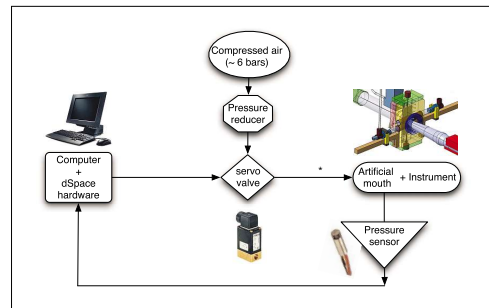


Figure 2: Principle of the pressure controlled artificial mouth.

minimize the difference between the measured and the target mouth pressure.

The force applied by the lip on the reed has also an influence on the value of the oscillation threshold. Analytical/numerical work presented in the companion paper assumes that this force is constant. Therefore, in order to compare the analytical/numerical results and experimental ones, this force is maintained constant during the experiment. For this, an artificial lip is used and its position is locked (cf. Figure 3)

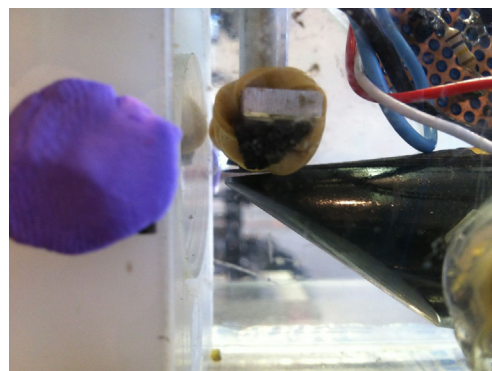


Figure 3: Lateral view of the mouthpiece placed in the artificial mouth. We see the locked position of the artificial lip.

Finally, a flowmeter is placed at the entrance of the artificial mouth in order to measure the nonlinear pressure/flow characteristic F of the instrument.

4 Experiment

4.1 Description of the experiment

The procedure of the experiment is as follows: starting from a small value (0.2 kPa in our experiment) the mouth pressure P_m is increased at a constant rate (the slope) k , until a limit value beyond the oscillation threshold. The mouth pressure is then decreased. During the experiment, the mouth pressure P_m , the pressure in the mouthpiece P and the incoming flow U are recorded. The rms value P_{RMS} of the pressure in the mouthpiece is calculated.

Experiment is repeated for different values of the slope k and three times for each value. The value of the slopes are: 0.10, 0.14, 0.23, 0.76, 1.57 and 2.73 kPa/s. Figure 4 shows an example of the time profile of P_m , P and P_{RMS} with $k = 0.1$ kPa/s.

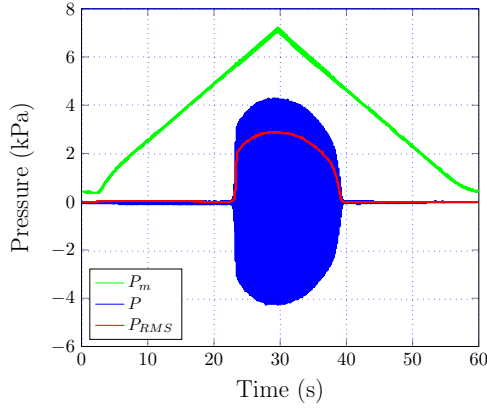


Figure 4: Time evolution of the mouth pressure P_m (green), the pressure inside the mouthpiece P (blue) and its rms value P_{RMS} (red). The slope k , of the mouth pressure is equal to 0.1 kPa/s.

4.2 Experimental results

The rms value P_{RMS} is plotted as a function of the mouth pressure P_m . Figure 5 highlights an hysteretic cycle: the value of P_m when the oscillations start during the increasing phase is larger than the value when the oscillations stop during the decreasing phase. This is a first difference with the static theory which predicts that these two values are the same and equal to the static oscillation threshold P_{mt} (case of a direct Hopf bifurcation). We can also notice that the stopping P_m value for decreasing pressure is close to the theoretical static threshold. The theoretical static threshold is obtained with equation (4). The parameter α is determined with equation (3) using the fundamental frequency of pressure P inside the mouthpiece. The parameters P_M and ζ are determined using the coordinate of the maximum $M(M_x, M_y)$ of the nonlinear characteristic measured with the smaller slope and for decreasing pressure [2, 17] :

$$P_M = 3M_x, \quad (6)$$

and,

$$\zeta = \frac{3\sqrt{3}}{2} \frac{Z_c}{P_M} M_y. \quad (7)$$

Numerical values are: $P_M = 10.3$ kPa and $\zeta = 0.172$.

We focus here on the birth of the oscillations for increasing mouth pressure. In this case, we can notice that the system begins to oscillate for blowing pressure larger than the theoretical threshold, this is the phenomenon of *bifurcation delay*. We can notice in Figure 5 and 6 that bifurcation delay increases with the slope k . To study the influence of the slope k , the value P_{up} of P_{RMS} corresponding to the point where the second branch of the *static* bifurcation diagram is reached (cf. [9] for the definition of the *static* bifurcation diagram) is determined for each slope (see Figure 6).

Then, the values of P_{up} are plotted as functions of the slope k (see Figure 7).

Figure 7 shows that P_{up} seems to increase linearly with the slope k . In section 5 these experimental results are compared to numerical simulation of equation (1).

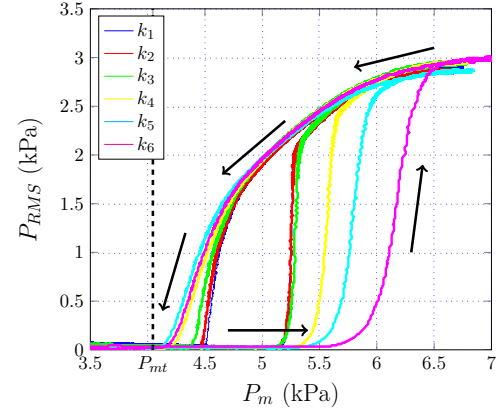


Figure 5: Graphical representation of P_{RMS} as function of P_m for different values of the slope k : $k_1 < k_2 < \dots < k_6$. Arrows represent the direction of the mouth pressure time evolution and highlight an hysteretic cycle.

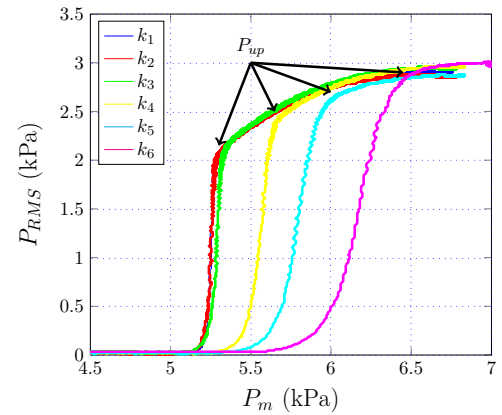


Figure 6: Part of the rms envelope P_{RMS} corresponding to the increasing mouth pressure and positions of P_{up} .

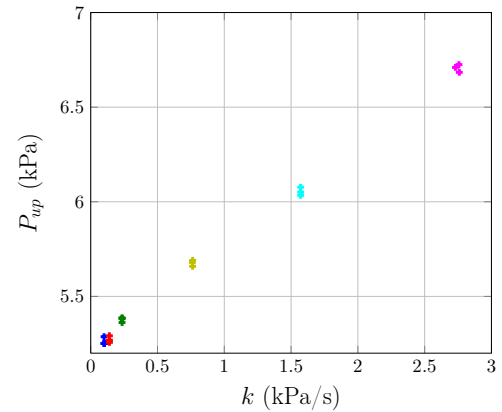


Figure 7: Graphical representation of P_{up} versus the slope k .

5 Comparison with simulations and discussion

In this section, previous experimental results (cf. Figures 5, 6 and 7) are compared to numerical computation of equation (1). Equation (1) is computed using the parameters P_M and ζ already estimated in Section 4.2. Firstly, the simulated P_{RMS} envelopes, obtained with the previous slopes are plotted in Figure 8. As in experiments, hysteric cycles and bifurcation delay are present in simulations. Except for

the cyan curve (corresponding to the slope k_5), in Figure 5 and just for decreasing blowing pressure, the influence of the slope of the blowing pressure is the same in both experimental and simulated systems and for both increasing and decreasing pressure.

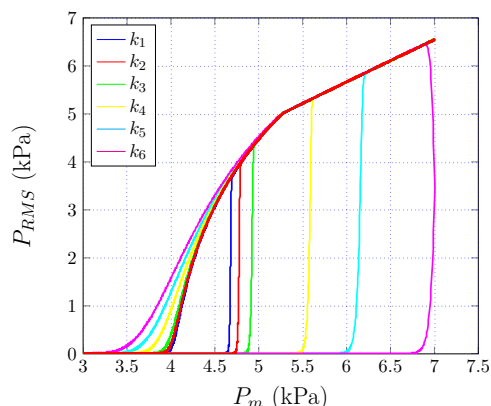


Figure 8: Graphical representation of simulated P_{RMS} as a function of P_m for the different slopes.

Companion paper [9], focused on increasing blowing pressure cases, shows that the precision (the precision is the number of digits used by the computer) used for the simulations has a very important influence on the bifurcation delay: the smaller the precision, the shorter is the bifurcation delay. Results presented in Figure 8 are calculated in *Matlab*® with a precision equal to 15 decimal digits.

Figure 9 shows a comparison between experimental values of P_{up} and simulated ones obtained with different values of the precision (the choice of the precision is possible using *mpmath*, the arbitrary precision library for *Python*).

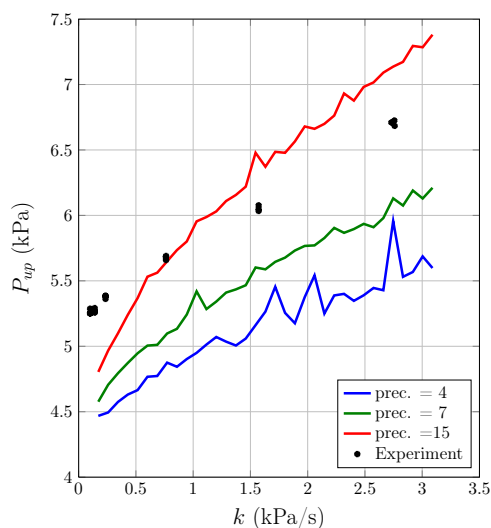


Figure 9: Graphical representation of P_{up} versus the slope k . Comparison between experiment and simulations.

The first observation we can do on Figure 9 is the very high dependence of the simulated P_{up} to the precision. We can notice that the slope of the curve $P_{up} = f(k)$ increases with the precision used. Quantitatively the evolution of both experimental and numerical P_{up} are the same: bifurcation delay ($\equiv P_{up}$) increase with the slope k of the mouth pressure. One would expect that the noise in experimental system corresponds to a low precision and therefore that bifurcation delay would be smaller. Figure 9 shows that it is not the case.

However, the slope of the experimental curve $P_{up} = f(k)$ seems to be closer to the numerical ones with $\text{prec.} = 4$ and 7. The offset might be imputed to the tough approximation in determining parameters P_M and ζ .

6 Conclusion

This work presented a preliminary study on the bifurcation delay in a clarinet. Static models for this instrument can predict the amplitude of the standing wave inside the bore as a function of the embouchure and the blowing pressure.

An artificial mouth in which the blowing pressure can be accurately controlled throughout time was used to play a simplified clarinet. With this device, the amplitude of the standing pressure wave inside the instrument was compared in two different conditions: first when increasing the blowing pressure from a value at which the instrument does not oscillate, and then when decreasing the pressure from an oscillating regime. In the latter case, the oscillation stops for a value close to what is predicted with static theory. For the increasing case however, the oscillation starts at a higher pressure value than this prediction. This value increases for higher rates of variation of the blowing pressure, revealing a phenomenon of bifurcation delay.

Although the pressure slopes used in this work are gentler than what can be obtained by a musician, these observations indicate that a sharp note attack probably requires the use of other parameters such as embouchure, vocal tract, or a more complicated profile of the blowing pressure (for example with an overshoot).

These results are similar to what is obtained in simulations based on Raman's model. Further work will focus on verifying this tendency for quicker pressure jumps and for more complicated time-evolutions of the pressure, including the use of an overshoot before stabilising the pressure.

Acknowledgments

This work was done within the framework of the project SDNS-AIMV "Systèmes Dynamiques Non-Stationnaires - Application aux Instruments à Vent" financed by *Agence Nationale de la Recherche*.

References

- [1] Jean-Pierre Dalmont, Joel Gilbert, Jean Kergomard, and Sebastien Ollivier. An analytical prediction of the oscillation and extinction thresholds of a clarinet. *J. Acoust. Soc. Am.*, 118(5):3294–3305, 2005.
- [2] Jean-Pierre Dalmont and Cyrille Frappe. Oscillation and extinction thresholds of the clarinet: Comparison of analytical results and experiments. *The Journal of the Acoustical Society of America*, 122(2):1173–1179, 2007.
- [3] T.A. Wilson and G.S. Beavers. Operating modes of the clarinet. *J. Acoust. Soc. Am.*, 56(2):653–658, 1974.
- [4] F. Silva, J. Kergomard, and C. Vergez. Interaction of reed and acoustic resonator in clarinet-like systems. *J. Acoust. Soc. Am.*, 124(5):3284–3295, 2008.

- [5] D. Ferrand, C. Vergez, and F. Silva. Seuils d'oscillation de la clarinette : validité de la représentation exciteur-résonateur. In *10ème Congrès Français d'Acoustique*. sfa.asso.fr, Lyon, April 12th-16th 2010.
- [6] A. Fruchard and R. Schäfke. Sur le retard à la bifurcation. In *International conference in honor of claude lobry*, 2007.
- [7] A. Fruchard and R. Schäfke. Bifurcation delay and difference equations. *Nonlinearity*, 16:2199–2220, 2003.
- [8] J. R. Tredicce, G.L. Lippi, P. Mandel, B. Charasse, A. Chevalier, and B. Picqué. Critical slowing down at a bifurcation. *American Journal of Physics*, 72(6):799–809, 2004.
- [9] B. Bergeot, A. Almeida, C. Vergez, and B. Gazengel. Attack transients in a clarinet model with time-varying blowing pressure. In *11ème Congrès Français d'Acoustique and 2012 Annual IOA Meeting*, Nantes, France, April 23th-27th 2012.
- [10] M. E. McIntyre, R. T. Schumacher, and J. Woodhouse. On the oscillations of musical instruments. *J. Acoust. Soc. Am.*, 74(5):1325–1345, November 1983.
- [11] J. Kergomard. Elementary considerations on reed-instrument oscillations. *Mechanics of musical instruments*, by A. Hirschberg/ J. Kergomard/ G. Weinreich. Volume 335 of *CISM Courses and lectures*:229–290., Springer-Verlag, Wien, 1995.
- [12] A. Hirschberg, R. W. A. Van de Laar, J. P. Mauries, A. P. J. Wijnands, H. J. Dane, S. G. Kruijswijk, and A. J. M. Houtsma. A quasi-stationary model of air flow in the reed channel of single-reed woodwind instruments. *Acustica*, 70:146–154, 1990.
- [13] A. Hirschberg. *Mechanics of musical instruments*. chap. 7, p. 291-369. N° 355 in CISM courses and lectures, Springer-Verlag, New York, 1995.
- [14] C. Maganza, R. Caussé, and F. Laloë. Bifurcations, period doublings and chaos in clarinetlike systems. *EPL (Europhysics Letters)*, 1(6):295, 1986.
- [15] J. Kergomard, J.-P. Dalmont, J. Gilbert, and P. Guillemin. Period doubling on cylindrical reed instruments. In *Proceeding of the Joint congress CFA/DAGA 04*, pages 113–114. Société Française d'Acoustique - Deutsche Gesellschaft für Akustik, 22th 24th March 2004, Strasbourg, France.
- [16] S. Ollivier, J. D. Dalmont, and J. Kergomard. Idealized models of reed woodwinds. part 2 : On the stability of two-step oscillations. *Acta. Acust. Acust.*, 91:166–179, 2005.
- [17] A. Chaigne and J. Kergomard. *Acoustique des instruments de musique*. Belin, 2008.
- [18] P.-A. Taillard, J. Kergomard, and F. Laloë. Iterated maps for clarinet-like systems. *Nonlinear Dynamics*, 62:253–271, 2010. 10.1007/s11071-010-9715-5.
- [19] J. Kergomard, S. Ollivier, and J. Gilbert. Calculation of the spectrum of self-sustained oscillators using a variable truncation method. *Acta. Acust. Acust.*, 86:665–703, 2000.
- [20] D. Ferrand and C. Vergez. Blowing machine for wind musical instrument : toward a real-time control of blowing pressure. In *16th IEEE Mediterranean Conference on Control and Automation (MED)*, pages 1562–1567, Ajaccion, France, 2008.
- [21] D. Ferrand, C. Vergez, B. Fabre, and F. Blanc. High-precision regulation of a pressure controlled artificial mouth : the case of recorder-like musical instruments. *Acta. Acust. Acust.*, 96:701–712, 2010.